Rare Met. (2015) 34(3):207–214
DOI 10.1007/s12598-014-0437-6

RARE METALS
www.editorialmanager.com/rmet

Intensified bioleaching of low-grade molybdenite concentrate by ferrous sulfate and pyrite

Juan Yu*, Hong-Ying Yang, Lin-Lin Tong, Jun Zhu

Received: 19 July 2014 / Revised: 18 November 2014 / Accepted: 19 December 2014 / Published online: 30 January 2015

Abstract Intensifying effects of ferrous sulfate and pyrite on bioleaching of low-grade molybdenite concentrate were studied in this paper. The experimental results show that the oxidation dissolution of molybdenite can be accelerated with the addition of either ferrous sulfate or pyrite in bioleaching medium. Pyrite has better enhancing effect than ferrous sulfate, and the highest molybdenum leaching rate in pyrite-added solutions is 20.85 %, increasing by 12.64 % compared with that in 9 K leaching system. Molybdenum leaching rate does not increase linearly with the increase of the addition of either ferrous sulfate or pyrite in each type solution. Great amounts of $[NH_4Fe_3(SO_4)_2(OH)_6]$ and $[KFe_3(SO_4)_2(OH)_6]$ with different morphologies will be deposited on molybdenite ores when the additions of Fe from ferrous sulfate or pyrite exceed that from 9 K leaching system by 0.5 times, and these deposits hinder the oxidation dissolution of molybdenite to some extent.

Keywords Low-grade molybdenite concentrate; Bio-oxidation; Intensified bioleaching; Ferrous sulfate; Pyrite

1 Introduction

Most types of molybdenite ores in nature inter-grow with porphyry copper ores or skarn type copper ores. As a result, molybdenite concentrates are usually obtained as by-products of separating flotation [1]. The process of roasting-ammonia leaching-purification is still the main technology in the industry of molybdenum extraction [2, 3]. However, the weaknesses of this traditional process gradually present due to the increasingly stringent requirements for the environmental protection and the characteristics of the available molybdenum resources becoming "poor," "fine," and "complicated" [4]. Hydrometallurgy processes have drawn increasing attention in recent years due to its excellent advantages of treating low-grade molybdenite ores. The hydrometallurgy processes for molybdenum extraction are mainly composed of oxidant leaching [5–7], oxygen pressure leaching [8], electric-oxidation extraction [9–12], and bioleaching [13–15]. Oxygen pressure leaching process usually performs under high-temperature high-pressure condition, and thus it proposes strict requirement for the reaction vessel. Meanwhile, its production process has hidden trouble in safety since the reaction processes are difficult to control. Compared with the reaction conditions of the oxygen pressure leaching process, those of oxidant leaching are relatively mild and the reaction processes are easy to control. Therefore, this technology has low cost in equipments. Nevertheless, the problem of high consumption of oxidant should not be neglected. The electro-oxidation process has the advantages of small equipment volume, convenient operation, and no requirement for oxidant. However, this technology also has the problem of high energy consumption and the evolution of harmful chlorine gas [16]. Bioleaching has the competitive advantages of mild operating condition, simple operation, and environmental cleaning. This technology is successfully applied in recovering Cu, Co, Ni, and U from low-grade ores or tailings, and it has a wild application prospect in recovering Ag, Cr, Ga, Mo, Pb, Pd, Pt, Rh, Ru, Sb, Zn, etc.,

J. Yu*, J. Zhu
School of Metallurgy Engineering, Xi'an University of Architecture and Technology, Xi'an 710055, China
e-mail: neuyujuan@163.com

H.-Y. Yang, L.-L. Tong
School of Materials & Metallurgy, Northeastern University, Shenyang 110004, China

from low-grade ores [17, 18]. It is considered that the recovery of Mo from molybdenite by bioleaching process is difficult because molybdenite has high chemical stability [19]. In recent years, plenty of researches in the field of bioleaching have been carried out to recovery molybdenum from molybdenum catalysts, low-grade molybdenite ores, and nickel–molybdenum sulfide ores [15, 20–22]. Nevertheless, bioleaching process is rarely used to treat low-grade molybdenite concentrate since molybdenum is a toxic metal ion to bacteria. It was reported that the oxidation of ferrous ion would be partly inhibited when the concentration of molybdenum ion reached 1 mmol·L^{-1}, and absolutely inhibited when it reached 2 mmol·L^{-1}. Gregory and Thomas [14] studied the effects of pulp potential, particle size, and temperature on the bioleaching of molybdenite concentrate. The experimental results indicated that the oxidation dissolution of molybdenite occurred with the potentials exceeding 505–555 mV vs.SCE (saturation calomel electrode) and molybdenum leaching rate increased with the decrease of particle size. Additionally, mesophilic bacteria were used to leach molybdenum from ultrafine molybdenite concentrates (10–13 μm) with grade of 7 %, and molybdenum leaching rate finally reached 85 % after 180 days. Abdollahi et al. [1] obtained the optimum conditions for the bioleaching of molybdenum, copper, and rhenium from high purity molybdenite concentrates with grade of 53.84 %. The experimental result showed that the optimum conditions of pH, solid concentration, and inoculation amount were 1.46, 1.88 %, and 18.41 %, respectively. Molybdenum leaching rate was 2.18 % after 20 days conducted under optimum conditions.

The way to strengthen molybdenum bioleaching efficiency includes domesticating molybdenum-tolerant bacteria, optimizing the bioleaching conditions and selecting suitable energy sources for bacteria. Pyrite and ferrous sulfate are commonly used as energy sources for bacteria. It was reported in many literatures that ferrous ions from pyrite and ferrous sulfate could be oxidized to ferric ions by bacteria in bioleaching medium. Then the molybdenite ores could be further oxidized by these ferric ions. Hence, pyrite and ferrous sulfate are used for intensifying the bioleaching of molybdenite ores. Askari et al. [13] found that the bacteria of Acidithiobacillus ferrooxidans were not poisoned by molybdenum ions and could grow well in solution containing 250 mol·L^{-1} molybdenum ions when pyrite was selected as bacterial energy source. Gregory and Thomas [14] reported that the bioleaching of molybdenite could be promoted by ferric ions. In this paper, ferrous sulfate and pyrites were selected as bacterial energy sources and a comparison study was conducted to investigate their intensifying effects on bioleaching of low-grade molybdenite concentrate.

2 Experimental

2.1 Ore sample

The ore sample used for this investigation was a certain low-grade molybdenite concentrate. The main metal mineral in this ore sample was molybdenite with a small amount of chalcopyrite. The chemical compositions of this molybdenite concentrate are shown in Table 1. The contents of Mo, Fe, and Cu are 25.4 wt%, 1.26 wt%, and 1.33 wt%, respectively; the elements of Mg, Ca, and Na also exist in ore sample. Granularity distribution of ore sample was determined using Malvern laser particle size analyzer and the analysis results are listed in Table 2. The particle size of ore sample is small and the ores with size of lower than 42 μm account for 85.38 %.

2.2 Leaching bacteria

The mixed thermophilic leaching bacteria were provided by Biometallurgy Lab of Northeastern University, China. It has excellent characteristics of molybdenum tolerance and acidophilic after long-term domestication. Additionally, the bacteria grow well in the solution containing ferrous ions and sulfur.

2.3 Microorganism culture

The culture medium for bacteria was 9 K medium. Its composition is as follows: 3.00 g·L^{-1} $(NH_4)_2SO_4$, 0.10 g·L^{-1} KCl, 0.50 g·L^{-1} K_2HPO_4, 0.50 g·L^{-1} $MgSO_4{\cdot}7H_2O$, 0.01 g·L^{-1} $Ca(NO_3)_2$, 44.30 g·L^{-1}L $FeSO_4{\cdot}7H_2O$. All chemical reagents used in this study were analytical grade.

2.4 Experimental procedure

The bioleaching experiments were divided into two groups. The strengthening effect of ferrous sulfate on the bioleaching of low-grade molybdenite concentrate was investigated in Group I. 100 ml iron-free 9 K culture medium and different amounts of ferrous sulfate heptahydrate (Table 3) were firstly

Table 1 Chemical compositions of low-grade molybdenite concentrate (wt%)

Mo	Fe	Cu	S	Na	Ca	Al	K	Mg
25.40	1.26	1.33	10.50	4.50	1.67	0.98	0.22	6.60

Table 2 Granularity distributions of molybdenite concentrate

Particle size/μm	<42	42–74	>74
w/wt%	85.38	11.50	3.12

added into Erlenmeyer flasks (Solutions 1–6), respectively. Then 2 g low-grade molybdenite concentrate was added into each solution, and pH value of solutions was adjusted to 1.5 using sulfuric acid. Subsequently, 100 ml bacteria liquid with 50 % inoculation amount were added after the stationary growth stage of bacteria was reached. Finally, the Erlenmeyer flasks were put into the constant-temperature incubator under conditions of 44 °C shaking at 190 r·min^{-1}. The effect of pyrite on the bioleaching of low-grade molybdenite concentrate was investigated in Group II. Different amounts of pyrite and ferrous sulfate heptahydrate (Table 3) were added into Erlenmeyer flasks (Solutions 7–11), respectively. The rest procedures were the same as those in Group I. In two group experiments, Fe contents in Solutions 1–11 Erlenmeyer flasks were calculated and the results are also shown in Table 3.

Solution pH, pulp potentials, and the concentrations of Fe^{2+} and Mo^{6+} were measured at different time intervals. All the potentials mentioned in this paper were referred to saturation mercury electrode (SCE).

2.5 Measurement

Pulp pH and pulp potentials were measured using the Leici PHS-2F pH meter. The concentrations of Fe^{2+} were determined by the potassium dichromate titritimetric method [23]. The concentrations of Mo^{6+} were analyzed by thiocyanate spectrophotometry with TU-1901 UV ultraviolet photometer. The morphologies and compositions of bioleaching residues were investigated by Shimadzu SSX-550 scanning electron microscope (SEM) equiped with energy dispersive spectrometer (EDS).

3 Results and discussion

3.1 Variations of concentrations of Fe^{2+} and pulp potentials

The variations of Fe^{2+} concentrations ([Fe^{2+}]) and pulp potentials in ferrous sulfate-added solutions (Solutions 1–6) during bioleaching are shown in Fig. 1. As shown in Table 3, ferrous sulfate acts as the only bacterial energy source in Group I. The Fe contents in Solutions 1–6 are 0.75, 1.00, 1.25, 1.50, 2.00, and 2.50 times that in 9 K leaching system, respectively. It can be observed in Fig. 1 that the initial Fe^{2+}concentrations in various solutions increase with the increase of the addition of ferrous sulfate, whereas the initial potentials vary in opposite direction. Owing to that there is

Table 3 Fe contents in various Erlenmeyer flasks (g)

	Group I (Solutions 1–6)						Group II (Solutions 7–11)				
Erlenmeyer flasks	1	2	3	4	5	6	7	8	9	10	11
$FeSO_4·7H_2O$	2.21	4.43	6.65	8.86	13.29	17.72	0	4.43	4.43	4.43	4.43
FeS_2	0	0	0	0	0	0	1.91	0.96	1.91	3.83	5.74
Fe from $FeSO_4·7H_2O$	0.45	0.89	1.34	1.79	2.68	3.57	0	0.89	0.89	0.89	0.89
Fe from FeS_2	0	0	0	0	0	0	0.89	0.45	0.89	1.79	2.68
Fe from 100 ml bacterial liquid	0.89	0.89	0.89	0.89	0.89	0.89	0.89	0.89	0.89	0.89	0.89
Total Fe	1.34	1.78	2.23	2.68	3.57	4.46	1.78	2.23	2.67	3.57	4.46
Total Fe from 9 K leaching system	0.75	1.00	1.25	1.50	2.00	2.50	1.00	1.25	1.50	2.00	2.50

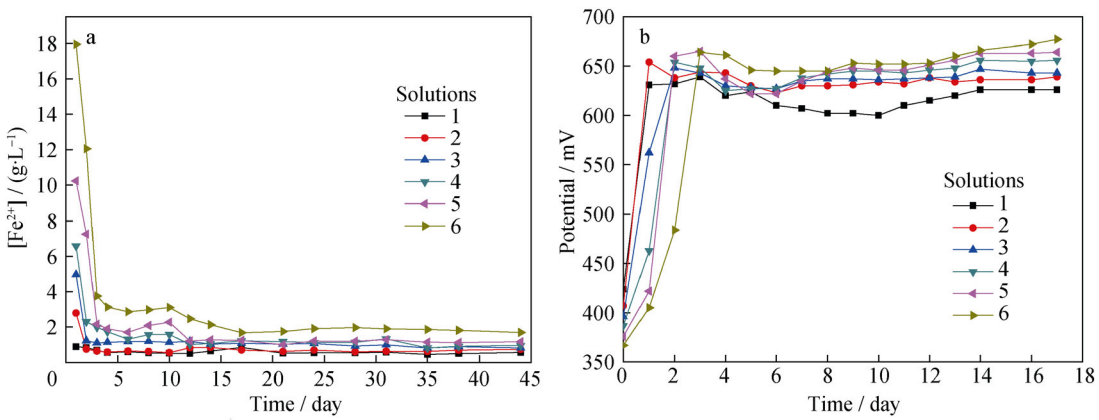

Fig. 1 Variations of [Fe^{2+}] **a** and pulp potentials **b** with bioleaching time in ferrous sulfate-added solutions

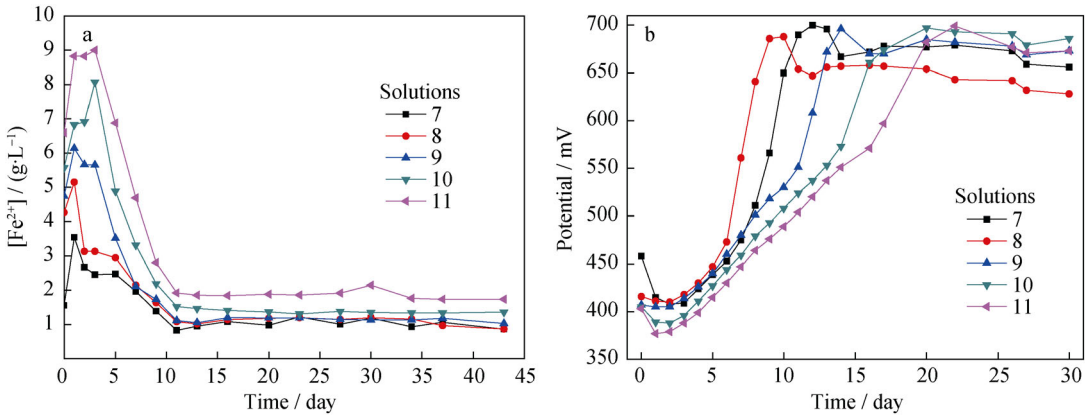

Fig. 2 Variations of $[Fe^{2+}]$ **a** and pulp potentials **b** with bioleaching time in pyrite-added solutions

relatively low addition of ferrous sulfate in Solutions 1 and 2, the Fe^{2+} are rapidly oxidized to Fe^{3+} in the 1st day, and the potentials of these two solutions quickly increase to 630 and 650 mV, respectively. After 2 days, the Fe^{2+}concentrations of Solutions 3–5 sharply decline from 4.96, 6.58 and 10.23 $g{\cdot}L^{-1}$ to 1.22, 2.31 and 2.17 $g{\cdot}L^{-1}$, respectively, and the potentials quickly increase to 650 mV. The rising rate of potential in Solution 6 is relatively slow since the initial Fe^{2+}concentration is high. Then, with the oxidation of Fe^{2+} to Fe^{3+} by bacteria, the Fe^{2+} concentration rapidly decreases within the initial 3 days, and the potential sharply increases to 660 mV. The Fe^{2+}concentrations in Solutions 1–6 gradually decrease with the process of bioleaching. The potentials of Solution 1, 2, 3–6 maintain at about 600–610, 630–640, and 640–660 mV in the residual time, respectively.

Figure 2 shows the variations of Fe^{2+} concentrations ($[Fe^{2+}]$) and potentials in pyrite-added solutions (Solutions 7–11) during bioleaching. As shown in Table 3, besides ferrous sulfate, different amounts of pyrite are added into the leaching solutions of Group II. The Fe contents in Solutions 7–11 are 1.00, 1.25, 1.50, 2.00 and 2.50 times that in 9 K leaching system, respectively. It is obvious that the changing trends of Fe^{2+} concentrations and potentials in pyrite-added solutions are different from those in ferrous sulfate-added solutions. In Solutions 7–9, Fe^{2+} concentrations rapidly increase in the 1st day with the dissolution of Fe from pyrite, and the potentials of these solutions gradually decrease due to the decrease of $[Fe^{3+}]/[Fe^{2+}]$ ratio. Subsequently, with the oxidation of Fe^{2+} to Fe^{3+}, Fe^{2+} concentrations decrease and pulp potentials gradually increase. Potentials of Solutions 7–9 reach 700 mV after 11, 9 and 14 days, respectively, when Fe^{2+} in solutions are almost oxidized to Fe^{3+}, and then slightly decrease and remain at 650, 630–650 and 680 mV, respectively in the residual time. In Solutions 10 and 11, Fe^{2+} concentrations increase rapidly within the initial 3 days due to that the additions of pyrite are relatively high. The pulp potentials decrease in the 1st day, and slightly increase in the next 2 days with the increase of $[Fe^{3+}]/[Fe^{2+}]$ ratio. Subsequently, the concentrations of Fe^{2+} rapidly decrease and the potentials of these two solutions gradually increase during the leaching process. The potentials of Solutions 10 and 11 increase to 700 mV after 20 and 22 days, respectively, and then remain at 670–680 mV in the residual time.

3.2 Variations of molybdenum leaching rates

3.2.1 Variations of molybdenum leaching rate in ferrous sulfate-added solutions

The variations of Mo leaching rates in solutions with different additions of ferrous sulfate are shown in Fig. 3. The results exhibit that there is the highest Mo leaching rate in Solution 4. Mo leaching rate in this solution increases rapidly in the initial bioleaching stage and reaches 7.68 % after 16 days. It slowly increases in the subsequent days and reaches 11.26 % after 34 days. Mo bioleaching rate remains constant in the residual time and finally reaches 11.57 %. Mo leaching rate in Solution 3 is a little lower than that in Solution 4 and finally reaches 10.87 %.The variations of Mo leaching rates in Solutions 1 and 2 have similar increasing trends, and Mo leaching rates finally reach 6.94 % and 8.21 %, respectively. Though there are relatively high additions of ferrous sulfate in Solutions 5 and 6, Mo leaching rates in these two solutions are lower than that in Solution 4 and finally reach just 9.80 % and 9.08 %, respectively.

It was reported that the oxidation dissolution of Mo from molybdenite concentrates occurred in bioleaching medium with potential exceeding 505–555 mV [14]. The additions of ferrous sulfate in Solutions 1 and 2 are relatively low, in which Fe contents are 0.75 and 1.00 times that in 9 K leaching system, respectively. As a result, the potentials of

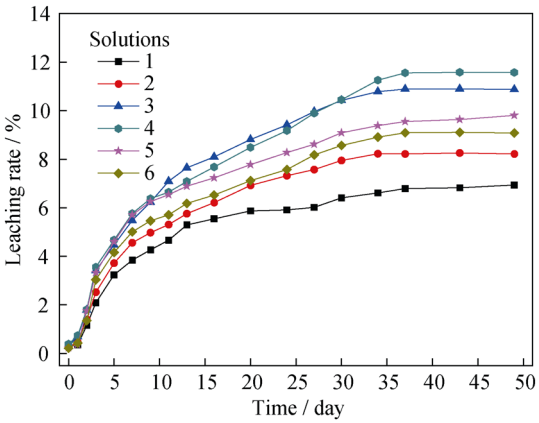

Fig. 3 Variations of Mo leaching rates with bioleaching time in ferrous sulfate-added solutions

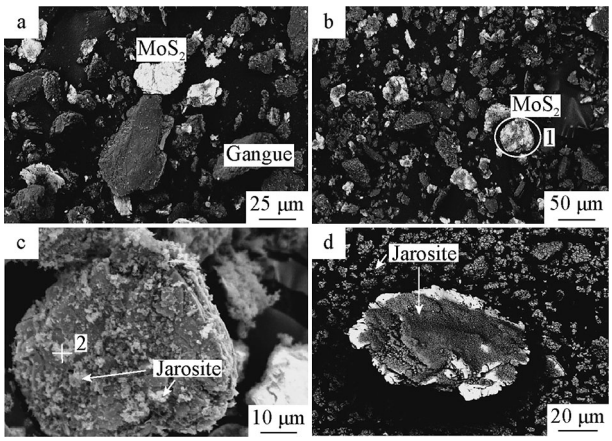

Fig. 4 SEM images of leaching residues after 49 days: backscattered electron image of ores from **a** Solution 4 and **b** Solution 5, **c** high magnification secondary electron image of Spot 1 in **b**, and **d** secondary electron image of ores from Solution 6

these two solutions are relatively low and correspondingly Mo bioleaching rates are just 6.94 % and 8.21 % after leaching, respectively. The potentials of Solutions 3 and 4 maintain at relatively high level since there are sufficient Fe^{3+} in solutions. Therefore, Mo leaching rates in these solutions increase relatively and finally reach 10.87 % and 11.57 %, respectively. In Solutions 5 and 6, Fe contents are 2.0 and 2.5 times that in standard 9 K leaching system, respectively. The potentials of these two solutions maintain at high potentials of 650–660 mV after 2–3 days leaching due to that there are high additions of ferrous sulfate. However, Mo leaching rates in these solutions are much lower than those in Solutions 3 and 4. The results suggest that Mo bioleaching rate does not increase linearly with the increase of the additions of ferrous sulfate. Nevertheless, this conclusion is not in accordance with the point that high potentials are beneficial for increasing the Mo bioleaching rates from molybdenite concentrate. In order to further understand the reason for this, SEM was used to observe the morphologies of bioleaching residues.

SEM images of residues from Solutions 4–6 after 49 days bioleaching are shown in Fig. 4. It can be seen in Fig. 4a that few deposits can be observed on the surface of molybdenite ores from Solution 4. As shown in Fig. 4b, many superficial deposits are evident on the surface of molybdenite in Solution 5. Figure 4c is the high magnification image of Spot 1 in Fig. 4b. It can be seen in Fig. 4c that the molybdenite ores are covered with bulk superficial deposits. Chemical composition of these deposits (Spot 2 in Fig. 4c) was analyzed by EDS. The analysis results (Fig. 5) show that the surface deposits are composed of Fe, S, O and K elements, which suggests that the superficial deposits are jarosite with chemical formula of $[MFe_3(SO_4)_2(OH)_6]$. The forming process of jarosite is according to the following chemical equations:

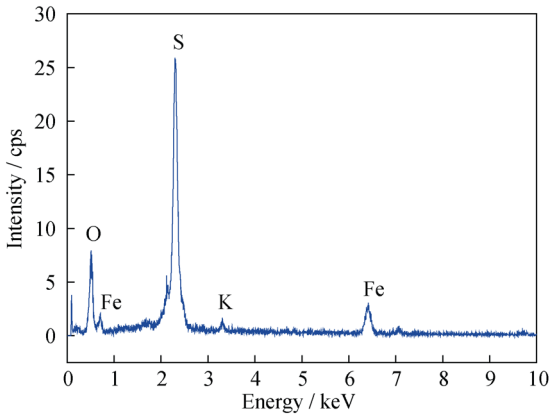

Fig. 5 EDS spectrum for deposits on surface of leaching residues from Solution 5

$$4Fe^{2+} + O_2 + 4H^{+} \xrightarrow{\text{Bacteria}} 4Fe^{3+} + 2H_2O \quad (1)$$

$$2Fe^{3+} + MoS_2 \longrightarrow Mo^{6+} + 2S^{-2} + 2Fe^{2+} \quad (2)$$

$$3Fe_2(SO_4) + M_2SO_4 + 12H_2O \Longleftrightarrow M_2Fe_6(SO_4)(OH)_{12} + 6H_2SO_4 \quad (3)$$

M in these equations represents the elements of K^+, Na^+, NH_4^+, Ag^+ or H_3O^+ [24, 25]. The chemical formula of jarosite formed on molybdenite ores may be $[NH_4Fe_3(SO_4)_2(OH)_6]$ and $[KFe_3(SO_4)_2(OH)_6]$ since there are bulk amounts of NH_4^+ and K^+ in culture medium. This kind of jarosite deposit restrains the diffusion of reactants and oxidation products through the precipitation zone, and it limits the oxidation dissolution rate of molybdenite with the effect of Fe^{3+} and bacteria. Therefore, Mo leaching rate in Solution 5 is lower than that in Solution 4. Likewise, superfluous Fe^{3+} in Solution 6 leads to the formation of

thick jarosite deposits on molybdenite particles as shown in Fig. 4d, which reduces Mo bioleaching rate in this solution.

3.2.2 *Variations of molybdenum leaching rates in pyrite-added solutions*

The variations of Mo leaching rates in solutions with different additions of pyrite are exhibited in Fig. 6. It can be observed that the processes of leaching in Solutions 7–11 can be divided into three stages, namely the initial stage, the middle stage and the later stage. In Solution 7, ferrous sulfate is not added and pyrite acts as the only bacterial energy source. Fe content in Solution 7 is equal to that in 9 K leaching system. Owing to that the activity of the bacteria and the potential are relatively low, Mo leaching rate increases slowly in the initial stage (1–9 days). As the time rises to the middle stage (10–30 days), the activity of the bacteria is enhanced after it get used to environment. Meanwhile, pulp potentials are relatively high. Mo leaching rate increases sharply in this stage and reaches approximately 8.75 % after 30 days. In the later stage (31–49 days), Mo leaching rate slightly increases due to the decline of the bacteria activity, and it finally reaches 9.64 %. With the addition of ferrous sulfate, the leaching initial stage of Solution 8 is shortened by 2 days compared with that of Solution 7. Mo leaching rate begins to significantly increase as time increases to middle stage (8–34 days) and reaches 18.06 % after 34 days. Then it slowly increases in the later stage (35–49 days) and finally reaches 19.63 %, much higher than that in Solution 7. The variation of Mo leaching rate in Solution 9 has similar trend as that in Solution 8. Owing to that there are higher additions of pyrite, the initial leaching stage of Solution 9 is prolonged by 2 days compared with that of Solution 8. Mo leaching rate begins to remarkably increase after 10 days leaching and finally reaches 20.85 % after 49 days, which is slightly higher than that in Solution 8. In Solutions 10 and 11, the initial stages are remarkably prolonged and correspondingly the middle stages are shortened. Mo leaching rates begin to significantly increase after 12 and 17 days, respectively, and reach 12.96 % and 13.11 % after 34 days. Then they slightly increase in later stage (35–49 days) and finally reach 14.63 % and 13.59 %, respectively, which are lower than that in Solution 9.

It is revealed from the analysis of Fig. 6 that the additions of pyrite in bioleaching solutions could obviously increase Mo leaching rate. Mo leaching rate in 9 K leaching system (Solution 2) is just 8.21 %. With different amounts of pyrite adding into 9 K leaching system, Mo leaching rates increase to 19.63 % (Solution 8), 20.85 % (Solution 9), 14.63 % (Solution 10) and 13.59 % (Solution 11), respectively. It could be concluded that Mo leaching rate does not increase linearly with the increase of the addition of pyrite and begins to decrease when the addition of Fe from pyrite exceeds that from 9 K leaching system by 0.5 times.

SEM images of ores from Solutions 10 and 11 after 49 days bioleaching are shown in Fig. 7. It could be seen in Fig. 7 that the molybdenite ores are covered with bulk jarosite deposits. Compared with the jarosite deposits on molybdenite from ferrous sulfate-added solutions, those from pyrite-added solutions show different morphologies. It could be concluded that when excessive pyrites are added in bioleaching solution, many bacteria will be in the state of oxidizing these bacterial energy sources, which reduces the bacterial oxidation efficiency. Additionally, the jarosite deposits restrain the oxidation dissolution of molybdenite during bioleaching.

3.2.3 *Comparison of enhancing effects of ferrous sulfate and pyrite on molybdenum bioleaching*

Mo leaching rates in pyrite-added solutions (Solutions 7–11) are higher than those in correspondent ferrous sulfate-added solutions (Solutions 2–6) with equal Fe contents. Mo leaching rates in Solutions 5–11 are relatively low due to the formation of bulk jarosite deposits on molybdenite ores. For all that, Mo leaching rates in pyrite-

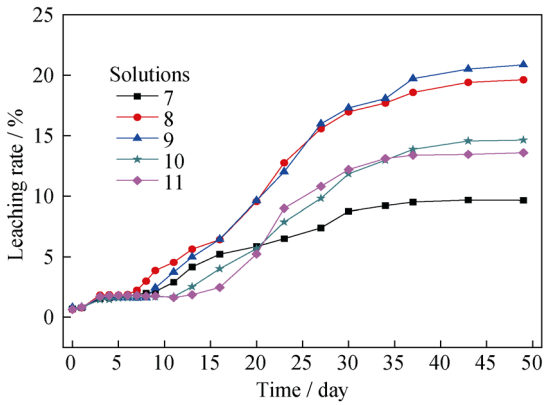

Fig. 6 Variations of Mo leaching rates with bioleaching time in pyrite-added solutions

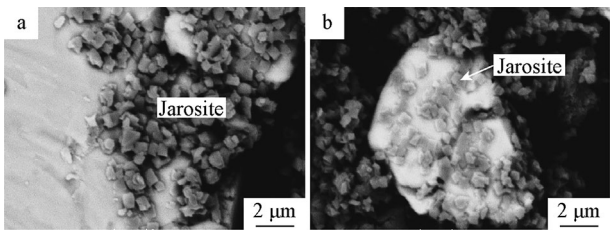

Fig. 7 SEM images of leaching residues after experiment: **a** Solution 10 and **b** Solution 11

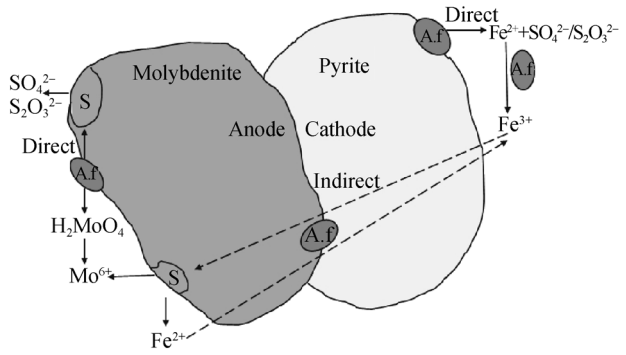

Fig. 8 Galvanic cell model of molybdenite/pyrite in bio-oxidation solution containing Acidithiobacillus ferrooxidans (a.f)

added Solutions 10 and 11 are still higher than those in ferrous sulfate-added Solutions 5 and 6. It could be concluded that the additions of pyrite have superior effect on increasing Mo leaching rates. There are two reasons for this. The first reason is related to the potentials of each type solutions. It is revealed from the results that the additions of either ferrous sulfate or pyrite in bioleaching solutions could increase pulp potentials to some extent. Potentials increase rapidly in the initial stage of bioleaching in ferrous sulfate-added solutions, but basically maintain at about 630 mV in the middle stage of bioleaching. As for the pyrite-added solutions, though the rising rates of potentials are relatively slow in the initial stage of bioleaching, potentials increase to 700 mV after certain days and maintain at about 680 mV in the residual time. Therefore, the additions of pyrite have superior effect on increasing pulp potentials during bioleaching. Secondly, rest potential of pyrite is higher than that of molybdenite in bioleaching solution, and the oxidation dissolution of molybdenite could be accelerated by the galvanic effect (Fig. 8).

4 Conclusion

The pulp potentials could increase to some extent with the additions of ferrous sulfate or pyrite in bioleaching solutions. As a result, both the energy sources have enhancing effect on increasing Mo bioleaching rate. The addition of pyrite has better effect that that of ferrous sulfate on increasing potential, and correspondingly the enhancing effect of pyrite is superior to those of other energy sources. The highest Mo leaching rates in ferrous sulfate- and pyrite-added solutions are 11.57 % and 20.85 % after 49 days, respectively, increasing by 3.36 % and 12.64 % compared with that in 9 K leaching system. Mo leaching rate does not increase linearly with the increase of the additions of ferrous sulfate and pyrite in each type solution. The formation of jarosite deposits on molybdenite particles restrains the oxidation process of molybdenite when the adding amounts of Fe from ferrous sulfate or pyrite exceed that from 9 K leaching system by 0.5 times.

Acknowledgments This study was financially supported by the National Natural Science Foundation of China (Nos. 51304151 and 51174062), and the High-Tech Research and Development Program of China (No. 2012AA061501).

References

[1] Abdollahi H, Shafaei SZ, Noaparst M, Manafi Z, Aslan N. Biodissolution of Cu, Mo and Re from molybdenite concentrate using mix mesophilic microorganism in shake flask. Trans Nonferrous Met Soc China. 2013;23(1):219.
[2] Yu J, Yang HY, Chen YJ, Fan YJ. Extraction of molybdenum from low grade molybdenum concentrates. J Northeast Univ (Nat Sci). 2011;32(8):1141.
[3] Deng GC, Xing NN, Li GF, Ju ZN, Ye LL. Effect of roasting fluxes for recovery of molybdenum on low grade molybdenum concentrate. J Liao Ning Univ (Nat Sci). 2009;36(4):349.
[4] Fu JG, Zhong H, Wu JL, Pu XM. Wet leaching of molybdenite at atmospheric temperature and pressure. Metal Mine. 2004; 12:35.
[5] Parsons GJ, Brimacombe JK, Peters E. Computer simulation of a molybdenite leaching process using dilute nitric acid. Hydrometallurgy. 1987;17(2):133.
[6] Vizsolyi A, Peters E. Nitric acid leaching of molybdenite concentrates. Hydrometallurgy. 1980;6(1):103.
[7] Gu H, Li HG, Liu MS. Study on new wet leaching of molybdenite. China Molybd Ind. 1997;10:29.
[8] Khoshnevisan A, Yoozbashizade H, Mozammel M, Sadrnezhaad SK. Kinetics of pressure oxidative leaching of molybdenite concentrate by nitric acid. Hydrometallurgy. 2012;111(2):52.
[9] Cao ZF, Zhong H, Liu GY, Qiu YR, Wang S. Molybdenum extraction from molybdenite concentrate in NaCl electrolyte. J Taiwan Inst Chem Eng. 2010;41(3):338.
[10] Cao ZF, Zhong H, Qiu ZH, Liu GY, Zhang WX. A novel technology for molybdenum extraction from molybdenite concentrate. Hydrometallurgy. 2009;99(1):2.
[11] Barr DS, Lindstorm RE, Hendrix JL. Control of the chlorate factor in electrooxidation leaching of molybdenum concentrates. Int J Miner Process. 1975;2(4):303.
[12] Barr DS, Scheiner BJ, Hendrix JL. Examination of the chlorate factor in electro-oxidation leaching of molybdenite concentrates using flow-through cells. Int J Miner Process. 1977;4(2):83.
[13] Askari ZMA, Hiroyoshi N, Tsunekawa M, Vaghar R, Oliazadeh M. Bioleaching of Sarcheshmeh molybdenite concentrate for extraction of rhenium. Hydrometallurgy. 2005;80(2):23.
[14] Gregory JO, Thomas RC. Bioleaching of molybdenite. Hydrometallurgy. 2008;93(1):10.
[15] Li CX, Luo YQ, Ren RC, Cheng Q, Man D. Enriching metal elements of carbonaceous molybdenum-nickel ore before leaching. Chin J Rare Met. 2013;37(2):289.
[16] Jia JP, Shen ZM, Zhou H. Development of electrochemical methods in waste water treatment. Shanghai Environ Sci. 1999; 18(1):29.
[17] Ehrlich HL. Past, present and future of biohydrometallurgy. Hydrometallurgy. 2001;59(2):127.
[18] Wu B, Wen JK, Chen BW, Yao GC, Wang DZ. Control of redox potential by oxygen limitation in selective bioleaching of chalcocite and pyrite. Rare Met. 2014;33(5):622.

[19] Cao ZF, Zhong H, Wen ZQ, Fu JG, Ding C. Research on ultrasonic electro-oxidation process of MoS_2 concentrate. J China Univ Min Technol. 2009;38(2):229.
[20] Chen JW, Gao CJ, Zhang QX, Xiao LS, Zhang GQ. Leaching of nickel-molybdenum sulfide ore with sulfolobus metallicus. Chin J Process Eng. 2009;9(2):257.
[21] Roya MG, Seyed MB, Seyyed MM. Bacterial leaching of a spent Mo–Co–Ni refinery catalyst using acidithiobacillus ferrooxidans and acidithiobacillus thiooxidans. Hydrometallurgy. 2011; 106(1):26.
[22] Pradhan D, Patra AK, Kim DJ, Chung HS, Lee SW. A novel sequential process of bioleaching and chemical leaching for dissolving Ni, V, and Mo from spent petroleum refinery catalyst. Hydrometallurgy. 2013;131(1):114.
[23] Tong LL, Yang HY, Zhang Y, Zhang GP. Effect of acid-ithiobacillus ferrooxidans on leaching out chalcopyrite and pentlandite. J Northeast Univ (Nat Sci). 2010;31(11):1591.
[24] Daoud J, Karamanev D. Formation of jarosite during Fe^{2+} oxidation by acidithiobacillus ferrooxidans. Miner Eng. 2006; 19(9):964.
[25] Jensen AB, Webb C. Ferrous sulfate oxidation using thiobacillus ferrooxidans: a review. Process Biochem. 1995;30(3):231.